ISSN (Print) : 0974-6846
ISSN (Online) : 0974-5645
Indian Journal of Science and Technology, *Vol 8(S8), 333–340, April 2015* DOI: 10.17485/ijst/2015/v8iS8/61920

A Novel Implementation of Image Segmentation for Extracting Abnormal Images in Medical Image Applications

K. Bharathi[1*] and S. Karthikeyan[2]

[1]Embedded System, Sathyabama University, Chennai - 600119, Tamil Nadu, India; bharathi3663@gmail.com
[2]Electronics and Communication, Sathyabama University, Chennai - 600119, Tamil Nadu, India; karthijoy1@gmail.com

Abstract

Background/Objectives: The main intent of this paper is to detect tumor in the mind by means of image segmentation. **Methods/Statistical Analysis:** The method used is fast border mark algorithm which is based on image segmentation. Image segmentation plays a crucial role in presentation of substantial shape and other areas of interest. The detection of tumor is based on horizontal and vertical score function using coefficient based on bhattacharya added with intensity histograms of gray level. The fast border marker algorithm is related with Intensity based border mark algorithm and Entropy based border mark algorithm. **Results:** The input consists of images of MR slices, and the output is to detect the abnormal area by means of pack which is oblong around the tumors. The method is based on training rule which is individually exchange recognition procedure which spots the section that is different between the two parts of the mind in MR slice using a vertical line. The detection exchange method has been using thresholding novelty found on function of bhattacharya intensity gray level histograms. The mean coefficients of dice for some patient conditions are less than 0.6 that meaningfully increases the scope for region-based border mark ability. The study consists of around ten MR images with a vertical line that moves across the mind. Different MR images may vary in area, form, position where we can still find the tumor in the mind. **Conclusion/Application:** The method is based on threshold segmentation. The segmentation technique uses fast border mark algorithm. The fast border mark algorithm is experimented on the MR images for finding the abnormal part in the mind.

Keywords: Brain Tumor, Detection of Brain Tumor, Image Segmentation, MRI Slice

1. Introduction

Now-a-days they are many medical centers that are maintaining huge data regarding the images about abnormal images. The behaviors of tumors are described based on different features like section, mode and location.

Image segmentation is the process of partitioning a digital image into multiple segments. The main intention of segmentation is to exchange the presentation of an image into something that can be understood more easily. Segmentation in image is to generally locate the target. In a correct manner, segmenting an image is to give a name to all the pixels in an image so that those pixels with the similar name are to divide based on definite characteristics. The output of segmentation is a collection of division parts that combined cover the entire image, or a set of contours extracted from the image (see edge detection). Based on certain features of pixels like color, intensity and texture they are divided.

*Author for correspondence

Some tumor segmented methods are not fully programmed as they need interface with the user to locate a seed inside the tumor[8,17]. Region growing is a simple region-based image segmentation method. The other name for region growing is pixel-based segmentation method where it includes how the basic points collection. The basic points are surveyed to check whether the basic points should be appended to it. In the similar way the operation is repeated, in the same manner as general data clustering algorithms. High time complexity is the disadvantage of Region growing[19]. The paper consists of an automated, speedy, and imprecise segmentation technique that consists of a rectangle box round the tumor which avoids the problems such as time complexity in region growing.

The algorithm consists of MR images as input where the tumor is located at different positions of the brain, and the output consists of oblong pack around the tumors. The axis of symmetry divides the brain into two parts with left part as the input image and the right part as the reference image. The output for the input image is it takes the input MRI image then finds the boundary of the brain and axis of symmetry. The vertical and horizontal score values are plotted against the number of days and growth rate if the two plots are dissimilar it detects the tumor. The vertical and horizontal score function uses the coefficient of bhattacharya which gives the similarity between two normalized intensity histograms. By using the centroids of the border marker method the unsupervised mean shift clustering[7] is implemented to find the largest cluster consecutive in MR slices.

The proposed function involves the novelty of the FBM segmentation technique which locates the border markers. The function is based on coefficient of bhattacharya[7] of intensity histograms which is gray scale. The coefficient is used to measure the similarities between two normalized histograms. It is defined as the square root of two histograms. Under reasonable conditions, the function admits a very speedy linear time search technique that locates the border markers. The advantages of FBM include: (a) no image registration is necessary, (b) dispensation of initial specification is not necessary, (c) no quality of intense in images are required and (d) it is a real time implemented.

2. Overview of the Proposed Work

The characteristics of the FBM system is described in section 3 next. Section 3.1 shows how the border markers are located around the tumors on MR images. Section 3 presents wide experimental studies. Section 4 describes the results and discussions.

3. Fast Border Mark Algorithm

FBM operates in two steps. The input set of images is individually processed, to find oblong pack firstly. In the second step, the border markers are grouped to spot the ones that are present around the tumor. It is based on the principle called unsupervised principle[2]. The outline of the above procedure is given in the following section.

3.1 Locating Border markers on 2D MR Slices

The following module describes about the idea behind FBM: D a region of change principle is obtained which is defined as the difference in-between the image to be tested I with the referral image R. In FBM, the a vertical line is drawn through the center of the image, the part on the left side has been regarded as the image of the test I, and the part on the right side as the image of the reference R. Now at this point D the region of change limited to be a rectangle box, which restricts the irregularity. To date most of the change detection methods is dissimilar from the region of change technique[24] for example. This change is viewed as a region-based as it varies based on more techniques. The thresholding function novelty is used to identify the D with two very fast searches one along the direction vertical and another across the horizontal of the picture.

Figure 1(a) the image to be tested and the referral image; have been shown with similar elevation and thickness subsequently i.e. h and w. The rectangular region is defined as the product of both horizontal and vertical parameters $D=[l_x,u_x]\times[l_y,u_y]$ detects the region of change/region of interest containing the tumor between the images I and R. The change in region found in FBM method have four not known features l_x, u_x, l_y and u_y. It first finds the best l_y and u_y values in a vertical range and then finds l_x and u_x in a horizontal range over the pair of images. In each range, the FBM algorithm uses a score function. Only the vertical score function is described and horizontal score function is taken as the transpose of vertical score function.

The vertical line represents linear axis of symmetry and the horizontal line divides the skull into four portions.

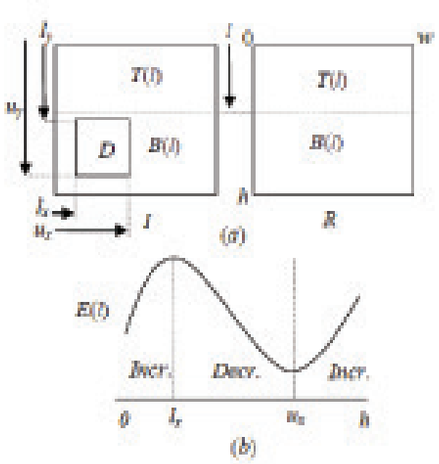

Figure 1. (a) To find out the change in region D from the input image I and referral image R. (b) Function plot of energy.

The line which is horizontal is shifted from top to bottom of the image and equation (1) is calculated for each position of the horizontal line. In the same manner, the vertical line is also moved and equation (1) is calculated accordingly and the tumor is located by a border mark.

Let $T(l)$ and $B(l)$ be respectively the "upper" and "lower" sub frames of the image, divided at a space l from the image tip: $T(l)=[0,w]\times[0,l]$ and $B(l)=[0,w]\times[0,h]$ (the rectangles intersecting at the dotted line drawn in Figure 1(a) as shown). We define our vertical score function as:

$$E(l)=BC\left(P_I^{T(l)},P_R^{T(l)}\right)-BC\left(P_I^{B(l)},P_R^{B(l)}\right) \quad (1)$$

Where $P_I^{T(l)}$ signifies the intensity histogram of image I which is normalized within the region $T(l)$.$P_R^{T(l)}$, $P_I^{B(l)}$, and $P_R^{B(l)}$ are defined accordingly. $BC(a,b)=\sum_i\sqrt{a(i)b(i)}\in[0,1]$

where BC (a, b) represents the Bhattacharya coefficient[10] between both the aligned graphs a (i) and b (i), and here i indicates a histogram bin. The Bhattacharya coefficient (BC) is used to find the similarity between two normalized intensity histograms. The applications of BC in various fields like tracking of the object[7], detection of edge[16], and registration[31] successfully. Here, we have:

$$BC\left(P_I^{T(l)},P_R^{T(l)}\right)=\sum_i\sqrt{\left(P_I^{T(l)}(i)\right)\left(P_R^{T(l)}(i)\right)} \quad \text{and}$$

$$BC\left(P_I^{B(l)},P_R^{B(l)}\right)=\sum_i\sqrt{\left(P_I^{B(l)}(i)\right)\left(P_R^{B(l)}(i)\right)}$$

If the two normalized histograms are the same, then BC is one and if the two normalized histograms between them are completely different the related BC value is 0. Thus, the score function $E(l)$. From Equation (1)) is large at the upper parts $T(l)$ when both the images are similar and the bottom regions $B(l)$ are dissimilar. Figure 2 shows $P_I^{T(l)}$, $P_R^{T(l)}$, $P_I^{B(l)}$, and $P_R^{B(l)}$ separately. So the tumor is located at the Bottom - Right quadrant of the image shown in Figure 2(a), value of $BC(P_I^{T(l)}, P_R^{T(l)})$will be high (close to 1) and value of will be low (close to zero) which indicates the value of $E(l)$ (equation1) is high.

Some of the properties of E (l) are proved, which locates the rectangle box D round the tumor. As the length varies from zero to height (h) the threshold function initially goes up and comes down and again goes up which is shown in Figure1(b). The segments at l = ly and l = uy, represents the maximum and higher bound of D separately. From the score function plot we can identify the

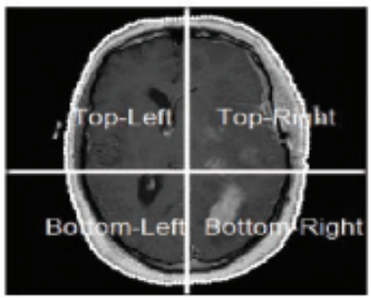

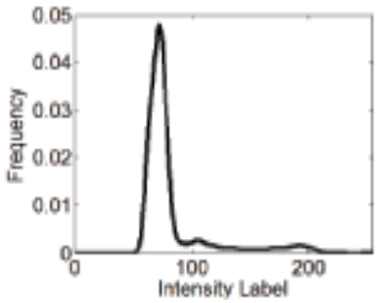

(b) Graph for Top - Left quadrant ($P_I^{T(l)}$).

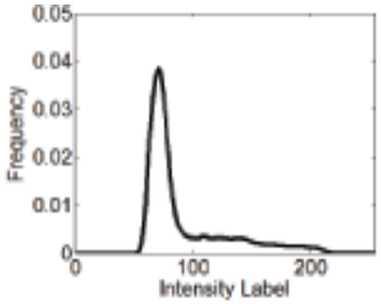

(c) Graph for Top - Right quadrant ($P_R^{T(l)}$)

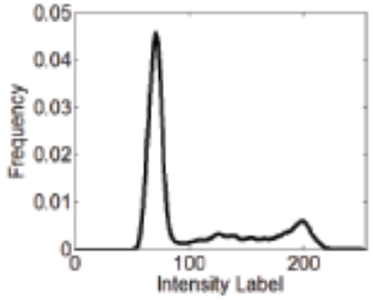

(d) Graph for Bottom - Left quadrant ($P_I^{B(l)}$)

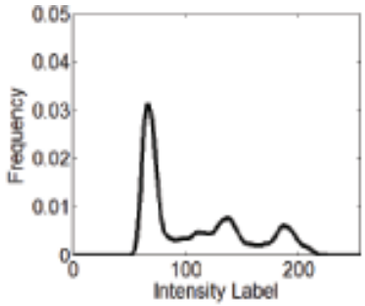

(e) Graph for Bottom - Right quadrant ($P_R^{B(l)}$)

Figure 2. The four quadrants represent the graphs. Gray-level histogram of Top - Left and Top - Right are same. However, gray - level histogram of Bottom - Left and Bottom - Right are different since tumor locates at Bottom - Right quadrant.

beneath and the top hops of change in region very easily. The part which is on the left with the part on the right edge of D subsequently represents lx and ux, which is recognized from threshold of horizontal plot. The resulting two schemes exactly begin the graph as it goes up down and once again goes up of energy nature ,given by particular constraint regarding image of the test, referral image and change in region. Initially, concept represents how the beneath and top of the edges of the threshold (1) in terms of D.

Concept 1: $U_D(l) \geq E(l) \geq L_D(l)$

$$U_D(l) = M_D(l) + \sqrt{\frac{|T(l) \cap D|}{|T(l)|}} BC\left(P_I^{T(l)\cap D}, P_R^{T(l)}\right) \quad (2)$$

$$L_D(l) = M_D(l) - \sqrt{\frac{|B(l) \cap D|}{|B(l)|}} BC\left(P_I^{B(l)\cap D}, P_R^{B(l)}\right) \quad (3)$$

$$M_D(l) = \sqrt{\frac{|T(l) \setminus D|}{|T(l)|}} BC\left(P_I^{T(l)\setminus D}, P_R^{T(l)}\right) - \sqrt{\frac{|B(l) \setminus D|}{|B(l)|}} BC\left(P_I^{B(l)\setminus D}, P_R^{B(l)}\right) \quad (4)$$

Proof: Let us write $P_I^{T(l)}$ as:

$$P_I^{T(l)} = \frac{|T(l) \cap D|}{|T(l)|} P_I^{T(l)\cap D} + \frac{|T(l) \setminus D|}{|T(l)|} P_I^{T(l)\setminus D} \quad (5)$$

for any set D. BC is defined as the square root of the interior product of functions which are two (here, normalized intensity histograms).The equation 5 is used to represent the interior product with linear scale and graph, one can display:

$$BC\left(P_I^{T(l)}, P_R^{T(l)}\right) \geq \sqrt{\frac{|T(l) \setminus D|}{|T(l)|}} BC\left(P_I^{T(l)\setminus D}, P_R^{T(l)}\right), \text{ and}$$

$$\sqrt{\frac{|T(l) \setminus D|}{|T(l)|}} BC\left(P_I^{T(l)\setminus D}, P_R^{T(l)}\right) + \sqrt{\frac{|T(l) \cap D|}{|T(l)|}} BC\left(P_I^{T(l)\cap D}, P_R^{T(l)}\right) \geq BC\left(P_I^{T(l)}, P_R^{T(l)}\right).$$

Both set of same variation enfold for $BC(P_I^{B(l)}, P_R^{B(l)})$. By joining the four variations gives the output.

Let us use Concept 1 to find the energy function as it goes up down and up again, threshold (1) as given in Figure 1(b). Following expectations are to be considered:

Assumptions:

(i) $BC\left(P_I^D, P_R\right) = \varepsilon$

(ii) $BC\left(P_I^{T(l)\setminus D}, P_R^{T(l)}\right) = c_1$

(iii) $BC\left(P_I^{B(l)\setminus D}, P_R^{B(l)}\right) = c_2$

where c_1 and c_2 are constant small numbers.

4. Results for Proposed Method

The results are simulated by using MATLABR2012A and the results involves axial brain MR image. MR images are taken as input for the simulation. The output for the input image is as shown above it takes the input MRI image then finds the boundary of the brain and axis of symmetry. The

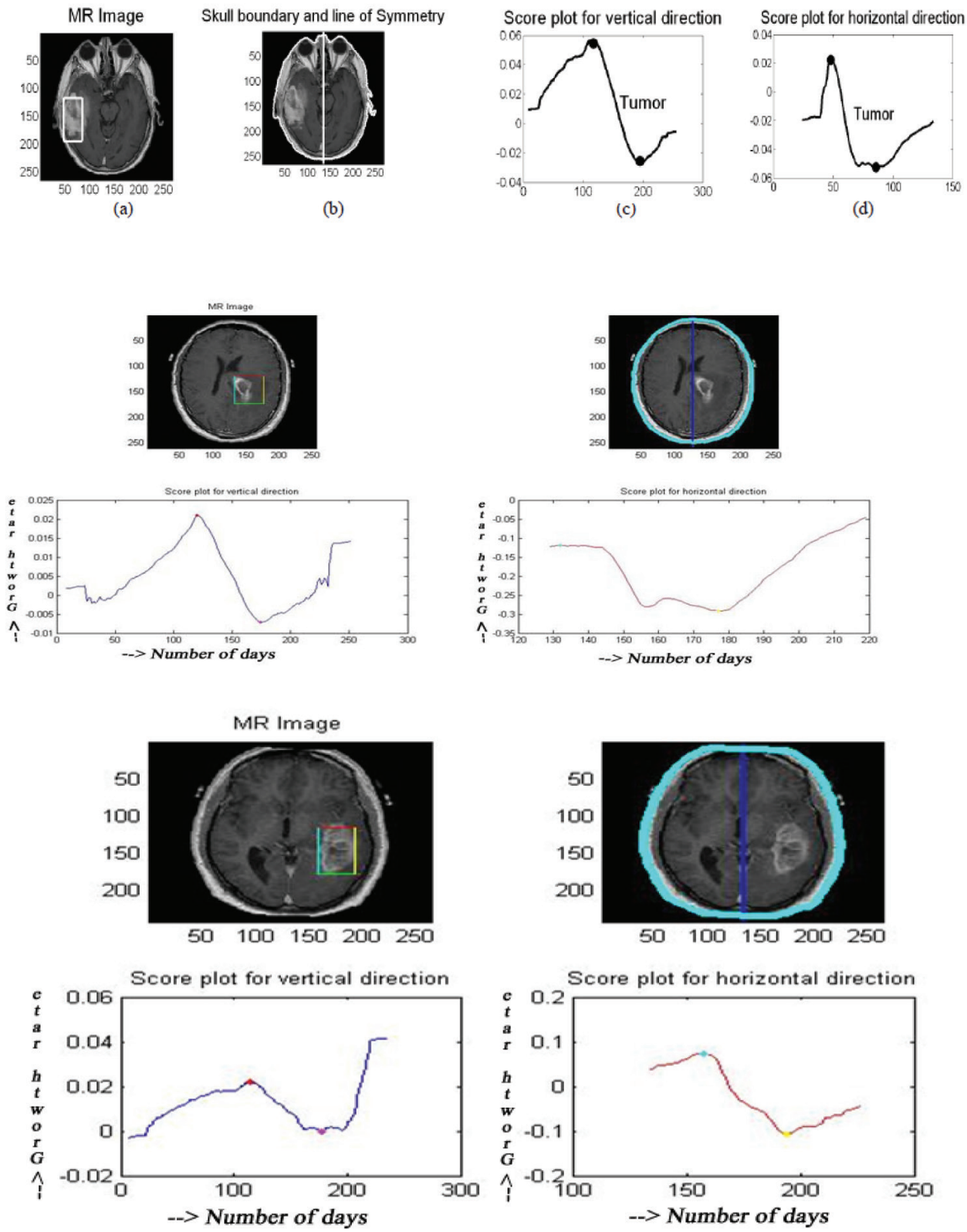

Figure 3. Locating brain tumor by the FBB method.

vertical and horizontal score values are plotted against the number of days and growth rate if the two plots are dissimilar it detects the tumor. One can understand from the outcomes of Proposition 1 and 2 easily some effects of BC and histograms which are normalized. From equation (4) it represents that the quantity M_D which is formed by collecting two dissimilar class of components which are separable: one is the geometric type: $\sqrt{\frac{|T(l)\setminus D|}{|T(l)|}}$ and $\sqrt{\frac{|B(l)\setminus D|}{|B(l)|}}$, and another type is the image intensity-based BCs. The splitting is achieved only by misusing: (a) inner product portion in BC and (b) the splitting portion nature of a graph which is normalized, i.e., equation (5). Intensity-based BC does not have much inequality in (4), the value of M_D can be resolved by using the two geometric components by using the before mentioned assumptions. The results of FBB method is compared with the IBB and EBB method. In FBB method we can detect the tumor correctly and exactly whereas in the other two methods we cannot detect the tumor exactly.

Figure 4(a) and Figure 4(b) illustrates how the abnormal area is detected using three methods for around ten patient images. The FBB system shows how correctly it can detect the abnormal area when compared to the other two systems though varying in area, form, position, direction and intensity.

The Coefficient of dice for the three systems i.e., FBB, IBB and EBB methods are compared[7] for all the images. Coefficient of dice is given by: $DC(b)=2|G\cap D(b)|/(|G|+|D(b)|)$ where D(b) is the set of pixels within the border mark found by b {FBB, IBB, EBB} algorithm and G is pixels along the border mark around the abnormal area.

4.1 Using Mean Shift Clustering in FBB Method

The MSC is used in FBB system to compute the potency and to differentiate the images with tumor from the rest of the image. The FBB is used to find the border markers on all the images independently and then the mean shift clustering is applied on FBB. The MSC groups all the abnormal images into one part and the remaining as different part. The mean for the patient studies have been computed using MSC method. The performance of MSC to differentiate the faulty from original images is shown in Table 1.

Table 1. MSC performance to differentiate faulty from original images

	Modality	Accuracy	Recall	Precision	F-measure
Tumor	T1C	92%	81%	97%	88%
Edema	T2	89%	92%	90%	91%

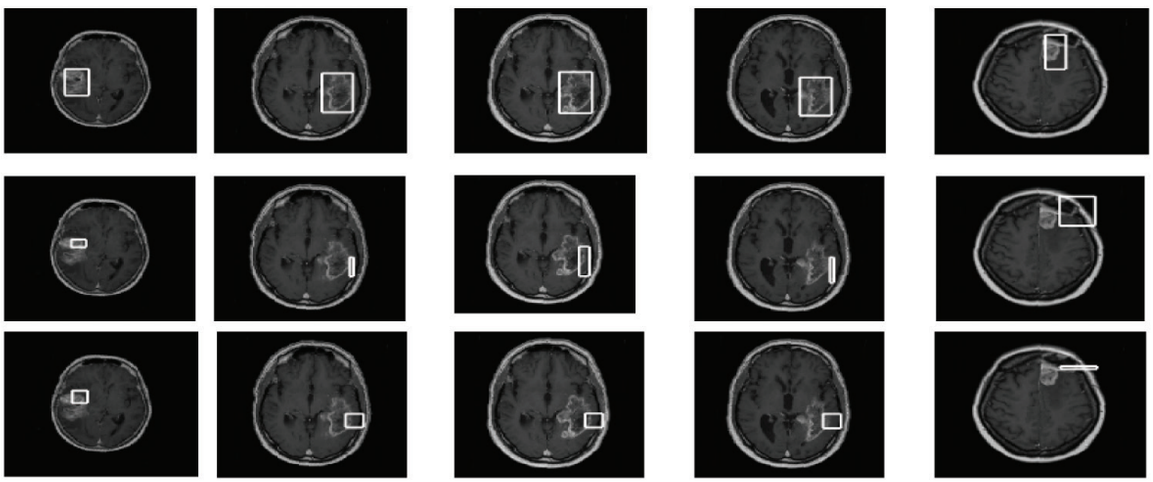

Figure 4(a). Axial brain MRI for T1C; First row shows the output for FBM system. Second row shows the output for IBM system. And the third row represents the output of EBM system.

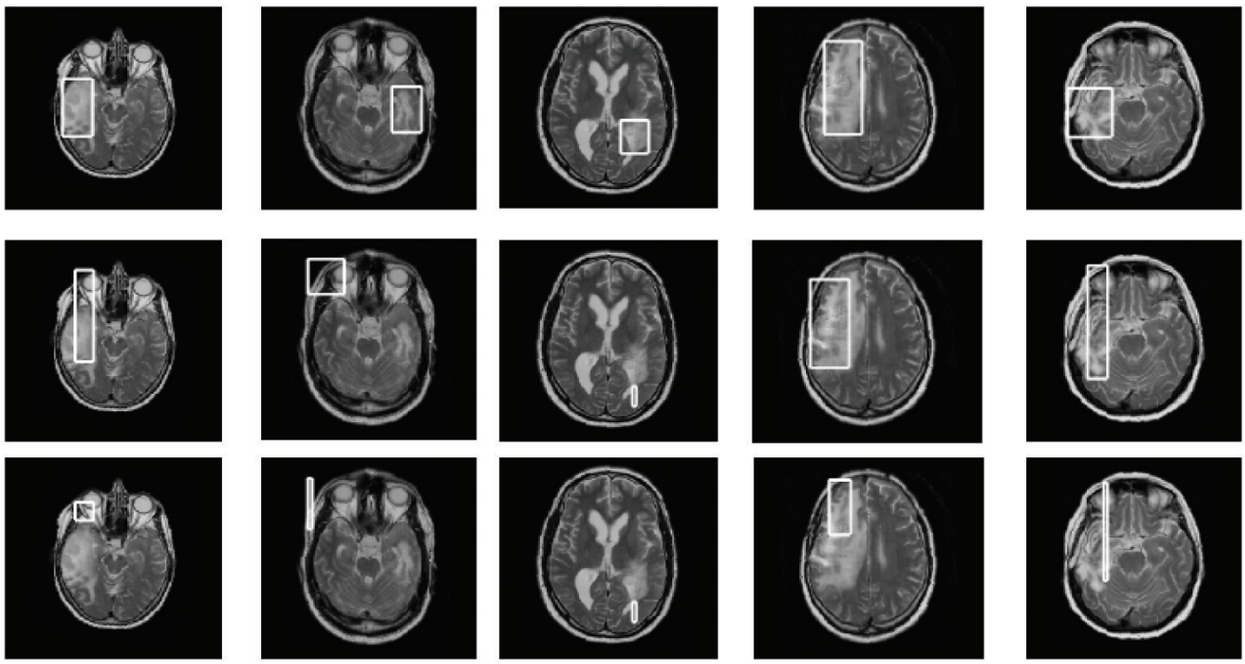

Figure 4(b). Axial brain MRI for T2; First row shows the output for FBM system. Second row shows the output for IBB system. And the third row represents the output of EBB system.

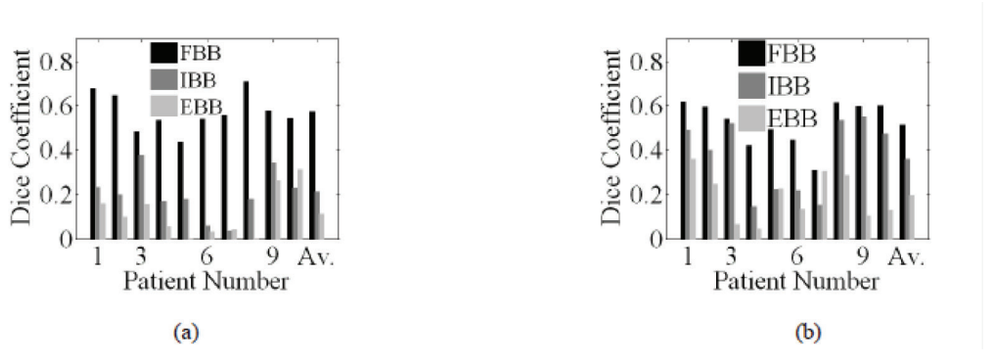

Figure 5. Coefficient of dices for different patients. "Av." indicates average. (a) T1C for tumor and (b) T2 for edema detection.

5. Conclusion

The paper consists of a FBM system which is a fast to detect the abnormal areas in the images. This method is fast, and is easy to implement when compared to the other methods which come under image segmentation technique. The Bhattacharya coefficient is used in the FBM model which is successfully implemented in other areas such as object tracking, edge detection, registration etc. The proposed method is also used to find the changes in intensities among different images. FBM can be implemented to find the kidney tumor and can be applied to ultrasonic and nuclear images as the future work.

6. References

1. Brummer ME, Mersereau RM, Eisner RL, Lewine RJ. Automatic detection of brain contours in MRI data sets. IEEE Transactions on Medical Imaging. 1993; 12(2):153–66.
2. Capelle AS, Alata O, Fernandez C, Lefevre S, Ferrie JC. Unsupervised segmentati on for automatic detection of brain tumors in MRI. Proceedings of International Conference on Image Processing; 2000. p. 613–6.
3. Caudra MB, Gomez J, Hagmann P, Pollo C, Villemure JG, Dawant BM, Thiran JP. Atlas-based segmentation of pathological brains using a model of tumor growth. Medical Image Computing and Computer Assisted Intervention, MICCAI; 2002. p. 380–7.

4. Chan TF, Vese LA. Active contour without edges. IEEE Transactions on Image Processing. 2001; 10:266–77.
5. Clark MC, Hall LO, Goldgof DB, Velthuizen R, Murtagh FR, Silbiger MS. Automatic tumor segmentation using knowledge-based techniques. IEEE Transactions on Medical Imaging. 1998; 17(2):187–201.
6. Karthikeyan S, Jayashri S. Energy utilization strategies using novel approach in wireless sensor networks. International Conference on Software Engineering and Mobile Application Modelling and Development; 2012 Dec. p. 1–5.
7. Clark MC, Hall LO, Goldgof DB, Velthuizen R, Murtagh FR, Silbiger MS. MRI segmentation using fuzzy clustering techniques. IEEE Engineering in Medicine and Biology. 1998; 17(2):187–201.
8. Comaniciu D, Ramesh V, Meer P. Real-time tracking of non-rigid objects using mean shift. Proceeding of CVPR; 2000. p. 142–9.
9. Dice LR. Measures of the amount of ecologic association between species. Ecology. 1945; 26(3):297–302.
10. Edward AA, Chihiro T, Michel JB, Andrew G, Saara T, Sven E. Accuracy and reproducibility of manual and semi automated quantification of MS lesions by MRI. J Magn Reson Imag. 2003; 17(3):300–8.
11. Fukunaga K. Introduction to statistical pattern recognition. 2nd ed. San Diego, CA, USA: Academy Press; 1990.
12. Hu Q, Nowinski WL. Radiological symmetry of brain and head images: Comparison and applications. Int J CARS; 2006. p. 75–81.
13. Hu Q, Nowinski WL. A rapid algorithm for robust and automatic extraction of the midsagittal plane of the human cerebrum from neuroimages based on local symmetry and outlier removal. Neuro Image. 2003; 20(4):2154–66.
14. Kaus MR, Warfield SK, Nabavi A, Chatzidakis E, Black PM, Jolesz FA, Kikinis R. Segmentation of meningiomas and low grade gliomas in MRI. Cambridge, UK: MICCAI; 1999.
15. Khotanlou H, Atif J, Colliot O, Bloch I. 3D brain tumor segmentation using fuzzy classification and deformable models. WILF; 2005. p. 312–8.
16. Khotanlou H, Colliot O, Bloch I. Automatic brain tumor segmentation using symmetry analysis and deformable models. Proceedings of International Conference on Advances in Pattern Recognition (ICAPR); 2007. p. 198–202.
17. Konishi S, Yuille A, Coughlan J, Zhu S. Fundamental bounds on edge detection: An information theoretic evaluation of different edge cues. IEEE CVPR; 1999. p. 573–9.
18. Lefohn A, Cates J, Whitaker R. Interactive, GPU-based level sets for 3D brain tumor segmentation. MICCAI; 2003.
19. Liu J, Udupa JK, Odhner D, Hackney D, Moonis G. A system for brain tumor volume estimation via MR imaging and fuzzy connectedness. Computer Medical Imaging Graphics. 2005; 29(1):21–34.
20. Lynn MF, Lawrence OH, Dmitry BG, Murtagh FR. Automatic segmentation of non-enhancing brain tumors in magnetic resonance images. Artif Intell Med. 2001; 21(1–3):43–63.
21. Michael RK, Simon KW, Arya N, Peter MB, Ferenc AJ, Ron K. Automated segmentation of MR images of brain tumors. Radiology. 2001; 218(2):586–91.
22. Moon N, Bulitt E, Leemput K, Gerig G. Model-based brain and tumor segmentation. Proceedings of International Conference on Pattern Recognition (ICPR); 2002. p. 528–31.
23. Otsu N. A threshold selection method from graylevel histogram. IEEE Transactions on System Man Cybernatics. 1979; SMC-9(1):62–6.
24. Prastawa M, Bullitt E, Ho S, Gerig G. A brain tumor segmentation framework based on outlier detection. Med Image Anal. 2004; 8(3):275–83.
25. Radke RJ, Andre S, Al-Kofahi O, Roysam B. Image change detection algorithms: A systematic survey. IEEE Transactions on Image Processing. 2005; 14(3):294–307.
26. Ray N, Russell G, Murtha A. Using symmetry to detect abnormalies in brain MRI. Computer Society of India Communications. 2008; 31(19):7–10.
27. Ray N, Saha B, Brown M. Locating brain tumor from MR imagery using symmetry. Proceedings of Asilomar Conference on Signals, Systems, and Computers; 2007. p. 224–8.
28. Ray N, Saha B, Zhang H. Change detection and object segmentation: A histogram of features-based energy minimization approach. Indian Conference on Computer Vision, Graphics and Image Processing (IEEE ICVGIP); 2008 Dec 16–19.
29. Sahoo PK, Soltani S, Wong AKC, Chen Y. A survey of thresholding techniques. Comput Vis Graph Image Process. 1988; 41(2):233–60.
30. Shi J, Malik J. Normalized cuts and image segmentation. IEEE Trans Pattern Anal Mach Intell. 2000; 22(8):888–905.
31. Sonka M, Hlavac V, Boyle R. Image Processing, Analysis, and Machine Vision. Third Edition. Boston, MA, United States of America: Brooks/Cole; 2008.
32. Viola P, Wells W. Alignment by maximization of mutual information. International Journal of Computer Vision. 1997; 24(2):137–54.
33. Silverman BW. Density estimation for statistics and data analysis. London: Chapman and Hall; 1986.
34. Wang Z, Hu Q, Loe K, Aziz A, Nowinski WL. Rapid and automatic detection of brain tumors in MR images. Proceeding of SPIE Medical Imaging. 2004; 5369:602–12.
35. Available from: http://www.cancerboard.ab.ca/Treatment/CancerCareFacilities/CCI/